Ab initio modelling of transition metals in diamond

2003 J. Phys.: Condens. Matter 15 S2913

(http://iopscience.iop.org/0953-8984/15/39/015)

INSTITUTE OF PHYSICS PUBLISHING JOURNAL OF PHYSICS: CONDENSED MATTER

J. Phys.: Condens. Matter **15** (2003) S2913–S2927 PII: S0953-8984(03)66725-1

Ab initio modelling of transition metals in diamond

M Watkins and A Mainwood

Department of Physics, King's College London, Strand, London WC2R 2LS, UK

Received 30 July 2003
Published 19 September 2003
Online at stacks.iop.org/JPhysCM/15/S2913

Abstract

Transition metals (TM) from the first transition series are commonly used as solvent catalysts in the synthesis of diamond by high pressure, high temperature processes. *Ab initio* calculations on these metals, in finite clusters of tetrahedrally coordinated carbon, enable us to investigate trends in their stability and properties. By carrying out systematic studies of interstitial, substitutional and semi-vacancy TM defects, we show that the electronic structure of the TMs is complicated by the presence of 'dangling bonds' when the TM disrupts the crystal lattice: interstitial defects conform to the Ludwig–Woodbury (LW) model, whilst substitutional and semi-vacancy defects move from approximating the LW model early in the transition series to approaching the vacancy model for the heavier metals. Multi-configurational self-consistent field methods allow genuine many-electron states to be modelled; for neutral interstitial, and all substitutional TMs, the crystal fields are found to exceed the exchange energies in strength. Consequently, low spin states are found for these defects. We find substitutional defects to be the most stable, but that semi-vacancy TMs are very similar in energy to the substitutional defects late in the transition series; interstitial defects are only metastable in diamond. Given appropriate charge compensators neutral and positively charged interstitial TM defects were stable, while negatively charged species appeared to be strongly disfavoured.

1. Introduction

Transition metal (TM) impurities in diamond have been the subject of much experimental work, principally using the techniques of optical spectroscopy and electron paramagnetic resonance (EPR). However, systematic studies of TM impurities are much scarcer [1–3] and work has tended to concentrate on elucidating the structure of specific experimental data. A recent study [4] has carried out a survey of the properties of the first-row TM impurities within the local density approximation (LDA) formulation of density functional theory.

Most of the known optical and EPR centres are based on nickel, with three cobalt defects also detected. There is unconfirmed EPR evidence for Mn [5] and Cu [6] and the assignment of Fe_i^+ [7] is based on very circumstantial evidence. Ti [8, 9], Cr [8] and Zn [8] have been

0953-8984/03/392913+15$30.00

observed, but they were produced by ion implantation rather than as by-products of crystal growth and are of less interest. It is a real puzzle why other TMs, especially Fe and Cu, which are commonly used in the growth process, have not been positively identified as point defects in diamond.

It is believed that the TM initially enters the diamond lattice at either interstitial (TM_i) or substitutional sites (TM_s). These sites are strained as the TM is much larger than the carbon atoms forming the lattice, and when annealed at high temperatures neighbouring carbon atoms are ejected and the semi-vacancy defects form (TM_{sv}). In the semi-vacancy structure the TM occupies the mid-point between the two missing carbon atoms. Indeed it is inferred that the EPR centres NE1–9, which are believed to have a semi-vacancy structure, involve Ni because they appear as Ni_s^- anneals out [10].

Experimental data are generally interpreted within a qualitative or semi-empirical molecular orbital picture. These interpretations give a clear explanation of the interaction of the TM with the lattice, allowing qualitative discussion of trends in the properties of the TM defects.

In this paper the first-row TMs are studied using the Hartree–Fock formulation. Specifically the TMs at interstitial, substitutional and semi-vacancy sites in diamond have been modelled using the *ab initio* modelling package GAMESS [11]. The calculations facilitate the study of many properties of the TM defects, such as the binding energy of the TM in diamond, the accessibility of different charge states, energies of the optical transitions and equilibrium geometries. Trends in the change of these properties across the first transition series are examined and compared to other available calculations and experimental data. The use of the Hartree–Fock method rather than density functional theory allows more direct interpretation of the wavefunctions produced and allows calculated electronic configurations to be related to the models produced by analysing experimental data.

It is found that even approximate calculations can help elucidate the properties of TMs in diamond. More reliance can be placed on the calculations with larger clusters and/or better basis sets, but the qualitative results obtained from even the simplest calculations still stand. The ease of computation, furthermore, allows the transition series to be systematically investigated. Trends revealed by this method help interpretation of the electronic structure of the TM impurities; more accurate calculations on a smaller selection of defects would not have been as illuminating.

2. Methods

2.1. GAMESS

Calculations were performed using the PC GAMESS version [12] of the GAMESS (US) quantum chemistry package.

The calculations were carried out upon finite atomic clusters, terminated with hydrogen atoms, using Gaussian basis sets. Supercell calculations require much larger clusters to prevent interaction between the repeating units, and methods based upon plane-wave expansions of the wavefunction are inappropriate for such localized defects as TMs.

SCF calculations

The self-consistent field (SCF) calculations were carried out within the RHF (restricted Hartree–Fock) or ROHF (restricted open-shell Hartree–Fock) framework. The use of the ROHF formulation allows ‘state averaged’ SCF calculations to counteract a common problem

with defects of high symmetry, often referred to as 'charge sloshing': when degenerate or near-degenerate orbitals are present in the system, discontinuities in the energy can occur during the SCF cycle. This is countered by equally filling degenerate orbitals.

MCSCF (multi-configurational self-consistent field) calculations were used to allow high spin states and genuine excited states to be considered. These calculations were run without symmetry to ensure that all determinants were generated and this restricted the MCSCF calculations to small clusters.

Basis sets

The majority of the following calculations were carried out using a MINI [13] minimal basis set. Where explicitly stated a much better basis set was utilized to carry out the same calculations on the substitutional metal complexes. The basis sets used then were 6-31G [14] on the carbon atoms, TZV on the TM [15], which is a modified version of Wachters' original basis set [12] and a STO-3 basis set on the hydrogens [16, 17]. When used, this will be referred to as the TZV basis.

2.2. Clusters used

A variety of clusters were used in these calculations. For the interstitial defects a $TM_iC_{10}H_{16}$ cluster was used with a geometry optimized for Co_i^+ with a TZV basis set and a $TM_iC_{26}H_{30}$ cluster was used with a geometry optimized for Ni_i^0. Calculations based around a substitutional site were for the very small TMC_4H_{12} and the larger $TMC_{28}H_{36}$ clusters. The geometries for these clusters when calculations were not optimized were taken from calculation in a MINI basis of $Co_s^+C_4H_{12}$ for the smaller cluster and a calculation using a TZV basis set on $Fe_s^0C_{28}H_{36}$ for the larger cluster. A $TMC_{43}H_{42}$ cluster was used for calculations on TMs at semi-vacancy sites.

When calculating the binding energies of charged defects, several centres of general interest in diamond were calculated. The substitutional nitrogen, C centre, in $N_sC_4H_{12}$ clusters with both basis sets and in the larger $N_sC_{28}H_{36}$ clusters for the MINI basis set only: in a similar way, substitutional boron in $B_sC_4H_{12}$ and $B_sC_{28}H_{36}$ clusters were studied for the relevant charge states.

3. Electronic structure

The interpretation of experimental data from TM centres in diamond requires the identification of the valence orbitals of the defect. The valence orbitals control most of the impurity's properties when using optical or EPR methods. Two contrasting models are regularly used in this context, one due to Ludwig and Woodbury [18] and the other being the vacancy model [19]. These differ in the energetic ordering of the complex's orbitals (see figure 1).

The Ludwig–Woodbury (LW) model assumes that the metal's d orbitals are the highest energy occupied orbitals. Any dangling bonds, caused by the disruption of bonding in diamond by the TM, are filled with electrons transferred from the TM: the remaining electrons occupy orbitals largely formed from the TM 3d orbitals. For instance, when a TM occupies a substitutional site in diamond four sp^3 hybridized orbitals are left on the TM's four nearest-neighbour carbon atoms. Four of the TM's N electrons are transferred to fill these orbitals and $N - 4$ electrons are left to occupy the TM d orbitals.

The vacancy model assumes the opposite situation. The TM d orbitals lie lower in energy than the dangling bonds and the d orbitals are consequently filled by electrons. Any remaining

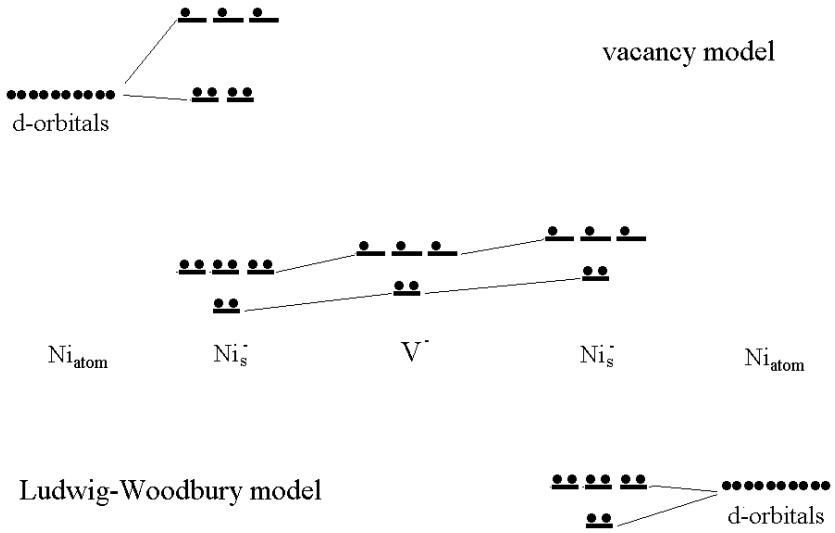

Figure 1. The electronic structure of Ni_s^- within the LW (left) or vacancy (right) paradigm.

electrons are housed in the dangling bonds. For a TM_s defect, the dangling bond orbitals resemble the orbitals of a vacancy in the diamond lattice.

Another consideration is the spin state of the TM: two opposing forces decide this. Exchange energy favours high spin states, with electrons having parallel spins. However, high spin states can only be achieved at the expense of promoting electrons into higher energy orbitals; where this cost in orbital energy outweighs the exchange energy contribution, low spin states are found.

3.1. Interstitial

The results of calculations on TM_i clusters illustrate an ideal LW electronic structure. Metal d orbitals are found in the bandgap and are split by the crystal field. All of the TMs were found to produce d-electron orbitals in the bandgap. Figure 2 shows the one-electron orbitals for the TM_i^+ complexes. Filling of these valence orbitals produces the observable many-electron states.

Spin states

MCSCF calculations found that the TM_i^0 species adopted low-spin electronic configurations, whilst the TM_i^+ complexes were found to be high spin (except V_i^+). Table 1 details the electronic configurations adopted and the energy difference from the lowest-energy alternative spin state. It can be seen that the low-spin configurations are found at the beginning of the series for the neutral clusters; this is in agreement with expectation if the splitting between metal orbitals is caused by covalent bonding with the relatively distant next-nearest-neighbour carbon atoms—the diffuse d orbitals at the beginning of the series have a good overlap with the ligand orbitals, resulting in large interactions between the orbitals. As the series is crossed, or when positive charge is added to the cluster, the d orbitals, which shield each other poorly from the charge, become much more localized on the metal and consequently their overlap with the ligand orbitals is significantly reduced. At the same time as the gap between the one-electron orbitals

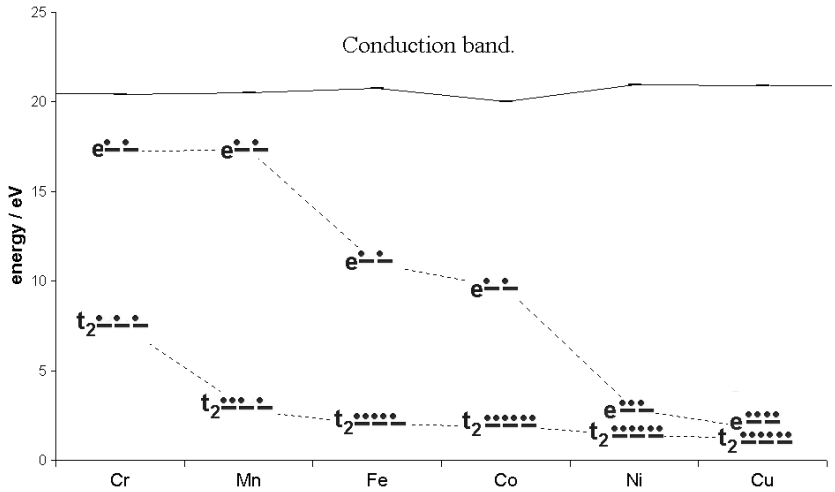

Figure 2. Electronic structure of the TM_i^+ series, showing the orbitals principally derived from the atomic TM 3d orbitals. Energies are relative to the top of the valence band.

Table 1. Ground state electronic configurations of TM_i. The energies of alternative ground states are also indicated. States arising from the strong-field model are in bold type.

	Ti	V	Cr	Mn	Fe	Co	Ni	Cu
TM_i^0	$(t_2)^4$	$(t_2)^5$	$(t_2)^6$	$(t_2)^6(e)^1$	$(t_2)^6(e)^2$	$(t_2)^6(e)^3$	$(t_2)^6(e)^4$	
Ground state	$\mathbf{^3T_1}$	$\mathbf{^2T_2}$	$\mathbf{^1A_1}$	$\mathbf{^2E}$	$^3A_2$	^2E	$^1A_1$	
Alternate	(+0.91)	(+1.55)	(+1.42)	(+0.08)				
Ground state	^5E	$^6A_1$	$^5T_2$	$^4T_2$				
TM_i^+		$(t_2)^4$	$(t_2)^3(e)^2$	$(t_2)^4(e)^2$	$(t_2)^5(e)^2$	$(t_2)^6(e)^2$	$(t_2)^6(e)^3$	$(t_2)^6(e)^4$
Ground state		$\mathbf{^3T_1}$	$^6A_1$	$^5T_2$	$^4T_1$	$^3A_2$	^2E	$^1A_1$
Alternate		(+0.44)	(+0.79)	(+0.05)	(+0.77)			
Ground state		^5E	$\mathbf{^2T_2}$	$\mathbf{^1A_1}$	$\mathbf{^2E}$			

is reducing, the electron–electron repulsion terms will increase as the orbitals become more localized. The crystal field splitting of 1.4 eV for the one known interstitial defect is not especially large and it is to be expected that these defects will be near the high-spin/low-spin crossing point.

3.2. Substitutional

In addition to metal d orbitals, dangling bonds are found in the bandgap. These orbitals are derived from the carbon sp^3 hybrids left unsaturated on the disruption of the crystal lattice by the TM.

The HF calculations suggest that the two common models (LW and vacancy) are extremes that are not met in practice. The metal d orbitals split under the crystal field into e and t_2 levels, whilst the 'vacancy' dangling bonds produce states of a_1 and t_2 symmetry. The vacancy model considers the metal orbitals to lie much lower in energy than the vacancy derived orbitals and the model of Ludwig and Woodbury presumes the opposite situation. To explain the electronic states obtained from Hartree–Fock calculations on substitutional TM clusters, it is necessary

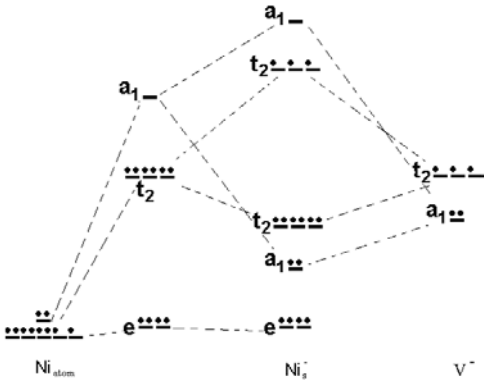

Figure 3. Molecular orbital diagram of Ni_s^-. The energy level structure shown is that obtained from the HF calculations in this paper. The formation of Ni_s^- is depicted as a negatively charged vacancy interacting with the neutral metal atom.

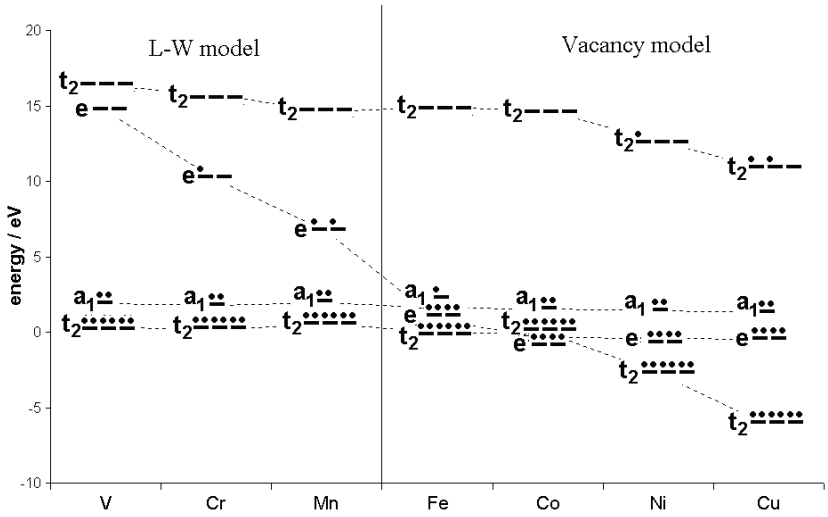

Figure 4. Orbitals of TM_s^+. The left hand side clearly shows behaviour typical of the LW model, but from Fe orbitals onwards the electronic configuration is qualitatively vacancy-like. Energies are measured relative to the valence band.

to consider the full set of states as the vacancy and metal orbitals often appear at comparable energies.

As the transition series is crossed, the metal orbitals come down in energy due to the incomplete screening of the additional nuclear charge. This effect suggests that the LW orbital model will be most accurate at the beginning of the transition series, and for the negatively charged substitutional complexes. Figure 4 shows this, but even for Ti_s^- it is found that covalent bonding is significant, where the metal t_2 orbital has 40% vacancy orbital character. As the series is crossed, the e orbitals drop sharply in energy, becoming lower in energy than the vacancy derived orbitals. However, the t_2 orbitals interact. This leads to an electronic scheme $(e)^4(a_1)^2(t_2)^6(t_2)^{N-8}$ or $(e)^4(t_2)^6(a_1)^2(t_2)^{N-8}$ for the later TM. For example, Ni_s^- (see figure 3) is found to have a ground state $(e)^4(a_1)^2(t_2)^6(t_2)^3$.

A further effect determines the ordering of the vacancy a_1 and t_2 orbitals. Previously the metal 4s level has been neglected; this is an old idea from crystal field theory, mainly dealing

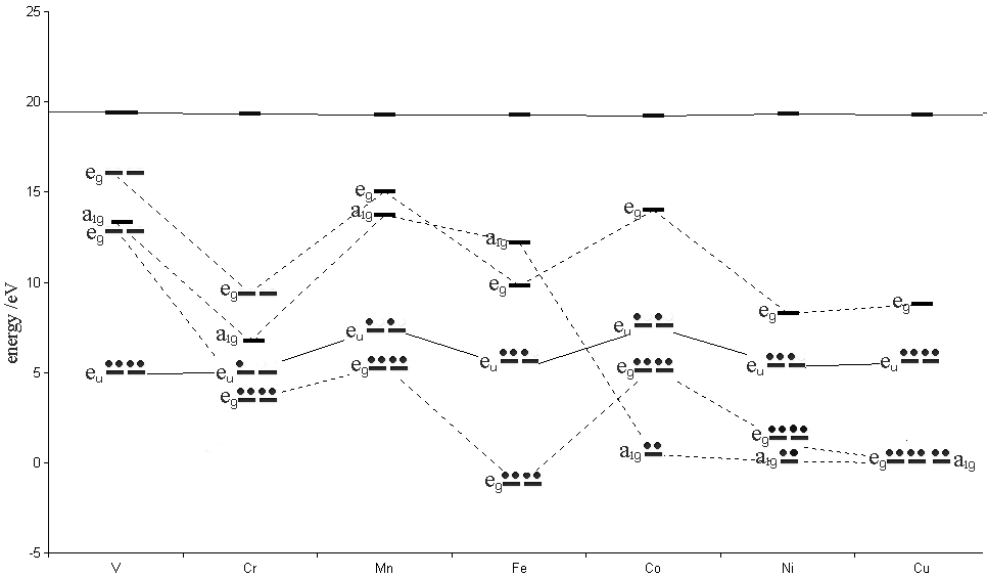

Figure 5. Orbitals of the TM_{sv}^{-} complexes. For clarity only the upper di-vacancy orbital is shown (e_u, joined by a full line). Energies are measured relative to the valence band. The conduction band is shown at the top of the diagram.

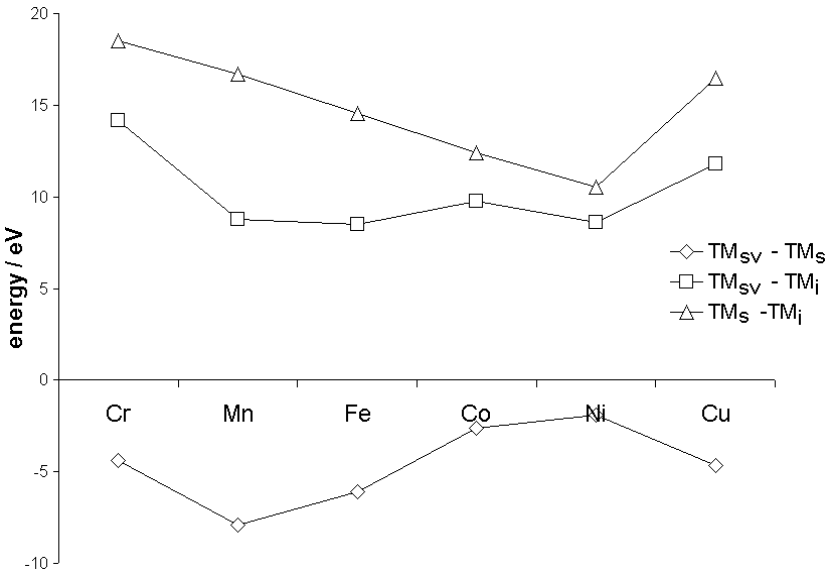

Figure 6. The binding energy differences between the different TM environments.

with positively charged complexes. As exterior and nuclear charges increase, the 3d electrons are stabilized much more strongly than other orbitals (particularly 4s) due to the charge being inefficiently screened. However, in TM_s^{-} complexes this argument does not hold and the 4s orbital can be involved in bonding interactions. In T_d symmetry it is of the same totally symmetric representation as the a_1 vacancy state, and can interact to form a strongly bonding

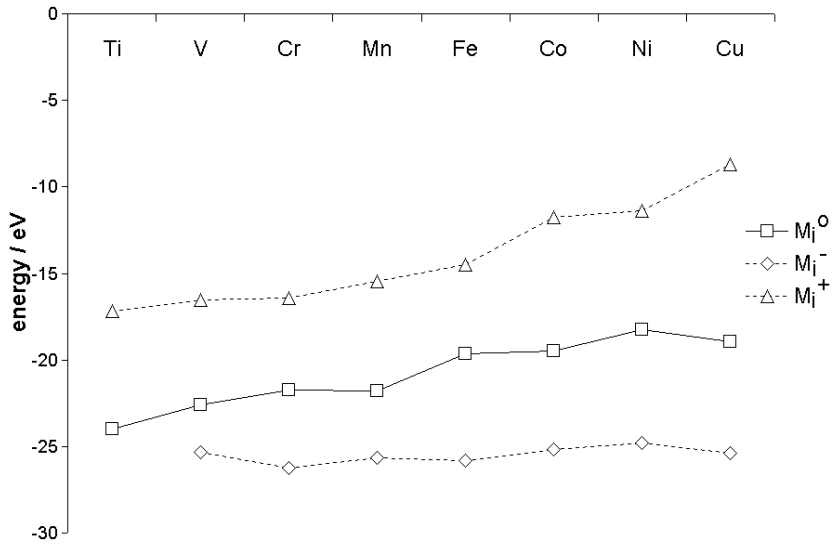

Figure 7. Binding energies of the $TM_iC_{10}H_{16}$ clusters in three charge states, including a +3.8 eV correction to charged clusters for finite cluster size (see the text).

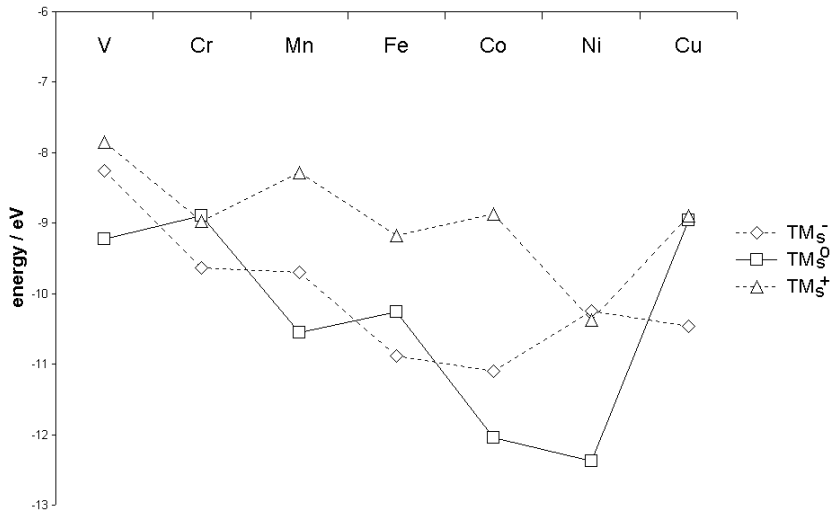

Figure 8. Binding energies of the $TM_sC_{28}H_{36}$ clusters including a +3.2 eV energy correction due to a finite cluster size for the charged species.

orbital. This leaves the a_1 state lower in energy than the vacancy t_2 orbitals for the negatively charged complexes.

For the neutral and positively charged complexes this ordering is reversed; the interaction with the metal 4s orbital stabilizing the a_1 state is reduced and the interaction between the two t_2 states increases. The resulting electronic configuration is $(e)^4(t_2)^6(a_1)^2(t_2)^{N-8}$, which corresponds qualitatively with the vacancy model (see figure 4).

The electronic states of the TM complexes are therefore found to change smoothly between approximating to the metal orbital model of Ludwig and Woodbury at the beginning of the

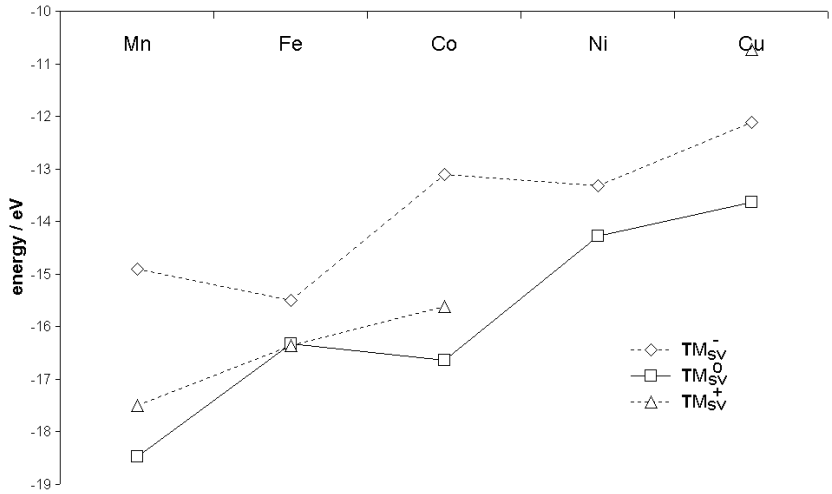

Figure 9. Binding energies of the $TM_{sv}C_{42}H_{43}$ clusters including a +3.0 eV energy correction due to a finite cluster size for the charged species.

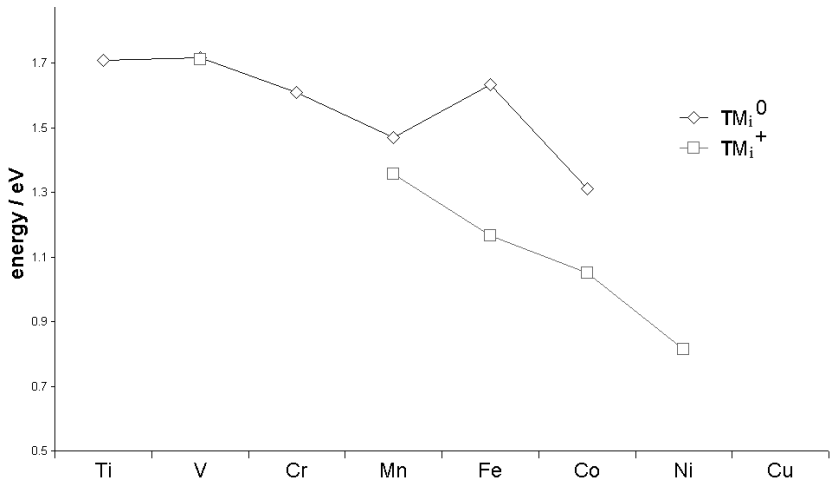

Figure 10. The transition energies found for the TM_i complexes.

transition series in negatively charged clusters, through to approaching the vacancy model for positively charged complexes at the end of the transition series. Furthermore the upper t_2 orbitals of the complex change in the same manner, being primarily derived from metal orbitals at the beginning of the series and becoming more vacancy-like as the series is crossed.

3.3. Semi-vacancy

A similar situation exists to that of the substitutional TMs. In the di-vacancy structure, the removal of two carbon atoms leads to a defect of D_{3d} symmetry and results in six dangling bonds, of a_{1g}, a_{2u}, e_g and e_u symmetry. The TM is assumed to occupy the centre of inversion of this structure and its d orbitals span a_{1g} and $2e_g$ irreducible representations of the point group. In the di-vacancy, calculations suggest that the dangling bond orbitals occur in order of increasing energy a_{1g}, a_{2u}, e_g and e_u [20]. However, current calculations suggest that the

Table 2. Electronic configurations of the TM_{sv} complexes. All have a $(e_g)^4(a_{1g})^2$ set of orbitals derived from the di-vacancy (not shown). Orbitals listed of gerade symmetry come principally from the TM, while those of ungerade symmetry are similar to di-vacancy orbitals. The many-electron state is shown in bold.

	Cr	Mn	Fe	Co	Ni	Cu
TM_{sv}^{+}		$(e_g)^4(a_{2u})^2(e_u)^2$ **$^3A_{2g}$**	$(e_g)^4(a_{2u})^2(e_u)^3$ **^2E_u**	$(e_g)^4(a_{2u})^2(e_u)^2$ **$^3A_{2g}$**	$(e_g)^4(a_{1g})^2(a_{2u})^2(e_u)^1$ **^2E_u**	$(e_g)^4(a_{1g})^2(a_{2u})^2(e_u)^2$ **$^3A_{2g}$**
TM_{sv}^{0}	$(a_{2u})^2(e_u)^4$	$(e_g)^4(a_{2u})^2(e_u)^1$ **^2E_u**	$(e_g)^4(a_{2u})^2(e_u)^2$ **$^3A_{2g}$**	$(e_g)^4(a_{1g})^2(a_{2u})^2(e_u)^1$ **^2E_u**	$(e_g)^4(a_{1g})^2(a_{2u})^2(e_u)^2$ **$^3A_{2g}$**	$(e_g)^4(a_{1g})^2(a_{2u})^2(e_u)^3$ **^2E_u**
TM_{sv}^{-}		$(e_g)^4(a_{2u})^2(e_u)^2$ **$^3A_{2g}$**	$(e_g)^4(a_{2u})^2(e_u)^3$ **^2E_u**	$(e_g)^4(a_{1g})^2(a_{2u})^2(e_u)^2$ **$^3A_{2g}$**	$(e_g)^4(a_{1g})^2(a_{2u})^2(e_u)^3$ **^2E_u**	$(e_g)^4(a_{1g})^2(a_{2u})^2(e_u)^4$ **$^1A_{1g}$**

ability of the metal d orbitals to mix in and increase the overlap in the *gerade* orbitals reduces their energy, giving an orbital ordering $e_g < a_{1g} < a_{2u} < e_u$. The question that needs to be addressed is whether the TM_{sv} complexes valence orbitals are di-vacancy-like or similar to the LW model.

The one-electron orbitals for the TM_{sv}^{-} complexes are shown in figure 5. V_{sv}^{-} is seen to approximate to the standard crystal-field model, the di-vacancy orbitals are filled and the unoccupied metal d orbitals lie at a higher energy; the metal orbitals are as expected for a slightly distorted octahedral environment: $e_g + a_{1g}$ at lower energy approximately degenerate and e_g at higher energy. The picture changes, however, as the transition series is crossed. The energy of virtual orbitals in the HF approximation is always too high, and when occupied it is found that the metal orbitals sink below the di-vacancy orbitals. Consequently it is found that all the TM semi-vacancy complexes' valence orbitals are di-vacancy-like. Physically this indicates that the orbitals involved are at similar energies and that electron–electron repulsions cause large changes to the one-electron orbitals, depending on the electronic configuration adopted.

Moving from V_{sv}^{-} to Cr_{sv}^{-} an extra electron must be accommodated. Instead of simply being placed into a metal e_g orbital to give a $(\text{divac})^{12}(\text{metal})^1$ configuration, it is found that the change in electron–electron repulsions strongly favours filling the metal e_g orbital at the expense of some of the di-vacancy orbitals to give a $(\text{divac})^8(\text{metal})^4(\text{divac})^1$ configuration. The di-vacancy orbitals then fill until it becomes preferable to occupy another metal orbital where again there is a balance between completely filling the metal orbital and leaving holes in the di-vacancy derived orbitals (favoured) or having partially occupied metal orbitals, which is found to be of higher energy in all cases. The metal a_{1g} becomes filled at Co onwards for all charge states whilst the second pair of metal e_g orbitals remain unoccupied.

The electronic configurations found are then $(\text{divac})^{12}(\text{metal})^0$ for V_{sv}^{-}, Cr_{sv}^{0} and $Mn_{sv}^{+}(\text{divac})^8(\text{metal})^6(\text{divac})^x$ for all charge states of Co, Ni and Cu and $(\text{divac})^8(\text{metal})^4(\text{divac})^y$ for all the other TM_{sv} complexes (table 2). The unpaired electrons always occupy a di-vacancy-like e_u orbital. This would make the observation of Ni hyperfine structure difficult to observe (figure 5).

Orbital occupations, and the many-electron states they give rise to, are shown in table 2. It can be seen that a very consistent set of ground states emerges from the fact that the di-vacancy-like e_u orbitals are always found to be the highest occupied molecular orbitals. Also, all the complexes are expected to be EPR-active except Cu_{sv}^{-}.

4. Binding energies

4.1. Methods

The binding energy of the TM is here considered to be simply the energy released from the system on placing the TM into the diamond lattice at the appropriate site. This definition means that the more positive the binding energy, the more strongly bound the TM, or the more thermodynamically favourable is its incorporation into the diamond lattice. This energy can be extracted from a Born–Haber cycle relevant to the exact system. Wherever possible, the energies of all species in the cycle are the internal energies from Hartree–Fock calculations, which are likely to be consistent within themselves. Occasionally empirical data must be used, such as for the cohesive energy of carbon in diamond. The exact terms used are presented in the relevant sections.

Generally, a single TM atom/ion will need to be included. In principle its total energy can be easily calculated. However, it is unclear what state the TM atom should be in during the calculation. The energy of the TM depends on two factors, its environment and electronic state (both of which make significant contributions to the value obtained for the binding energy).

The methods by which HPHT (high pressure, high temperature)-synthetic diamonds are prepared suggest that, rather than using an isolated TM ion as a reference, the metal in its liquid state should be used (or probably a saturated carbide of the metal at a high (but rather uncertain) temperature). Adequate data for the atomization energy of the metal liquids are, however, unavailable, and instead the isolated atom/ion is used as a reference to which is added the energy of atomization of the solid metal [21].

4.2. Comparison of TM environments

The stability of the different TM environments were compared, taking into account the differences in the number of carbon atoms in the various clusters. For example, to compare the stability of a TM_i in a $C_{10}H_{16}$ cluster with the same TM at a substitutional site in a $C_{28}H_{36}$ cluster we defined

$$\Delta H = E(TM_iC_{10}H_{16}) + E(C_{29}H_{26}) - E(C_{diamond}) - E(TM_SC_{28}H_{36}) - E(C_{10}H_{16}) \qquad (1)$$

and similar expressions for the other comparisons; the results are shown in figure 6.

The most immediate point is that the interstitial complexes are distinctly unstable relative to the other two environments—by around 10 eV for the Ni complexes. This is in agreement with the findings of Goss *et al* [22]. This suggests that interstitial complexes are only metastable in diamond. Certainly the transition to a substitutional site by pushing out a carbon atom along a ⟨111⟩ direction will be blocked by another carbon.

Substitutional complexes are found to be the most stable environment. This is in contradiction to the observations of Nadolinny *et al* [10]. However, the effects of long range stress induced by the presence of the TM impurity and entropic terms have been ignored in the present calculation: Johnston and Mainwood [3, 4] have suggested that strain in the crystal is reduced by around 1–2 eV by rearrangement to a semi-vacancy environment. The generation of a mobile carbon interstitial is likely to be entropically favoured. The magnitude of this effect is hard to estimate, but at the high temperatures at which the transition to the semi-vacancy structure occurs it could be substantial. Whilst speculative this shows that the results are not inconsistent with the experimental observation of the production of Ni_{sv}.

The relative stability of the semi-vacancy species increases quite sharply across the transition series, except for Cu. Ni_{sv} is about 2.5 eV more stable relative to Ni_s than the

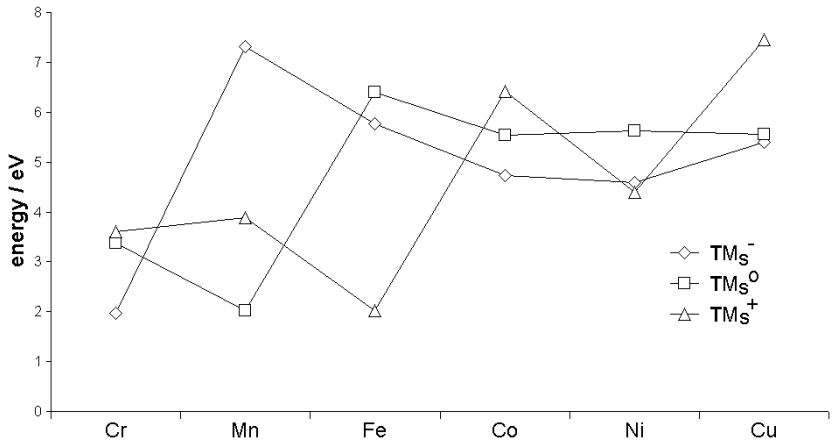

Figure 11. The transition energies of the TM_s complexes.

Co or Cu systems, with Fe another 1.5 eV less favourable. The other TM semi-vacancy species are less likely to be observed.

Relaxation

The equilibrium geometries of the TM complexes were found to change little across the series. All the centres in this paper have been relaxed in high symmetry point groups, T_d (TM_i and TM_s) and D_{3d} for the semi-vacancy, and the degrees of freedom for relaxation to occur in are limited. It was found that the energy changes on relaxation from a geometry obtained for $FeC_{28}H_{36}$ with a TZV basis set averaging only 0.2 eV for the $TM_sC_{28}H_{36}$ clusters with the MINI basis set. Similar results were obtained for the interstitial and semi-vacancy clusters.

Charge states

When considering different charge states, setting up a physically meaningful closed system is harder. 'Free' electrons or holes must be incorporated somewhere in the cycle, in an appropriate state. Doing this consistently is hampered by the fact that the position of the conduction and valence bands of the diamond shift, depending on the metal's environment and its charge state. Two methods have been used to accommodate the charged species: pinning the Fermi level to a certain energy below the conduction band (commonly that of the conduction band −1.7 eV nitrogen donor) or, as here, by incorporating another species in different charge states to model the process. We define the charging enthalpy for forming a charged cluster and charge compensating pair:

$$\Delta H^{+}_{\mathrm{CHARGE}} = E[(\mathrm{TM\ cluster})^{+}] + E[(\mathrm{B_sC_{28}H_{36}})^{-}] - E[(\mathrm{TM\ cluster})^{0}] - E[(\mathrm{B_sC_{28}H_{36}})^{0}], \tag{2}$$

$$\Delta H^{-}_{\mathrm{CHARGE}} = E[(\mathrm{TM\ cluster})^{-}] + E[(\mathrm{N_sC_{28}H_{36}})^{+}] - E[(\mathrm{TM\ cluster})^{0}] - E[(\mathrm{N_sC_{28}H_{36}})^{0}]. \tag{3}$$

Using these cycles has the advantage that all the terms involved are total energies calculated by the Hartree–Fock method and there is no need to resort to any empirical data. This does mean, however, that the relative stabilities of the charge states depend crucially on how well the references are modelled by GAMESS. It is anticipated that the simpler second row elements

used have been described at least as well as the TM. It is also hoped that errors due to finite cluster size will, to some extent, be cancelled by this method.

Another consideration for the charged species is the finite size of the clusters used in this survey. Charge in a crystal is screened by the response of the crystal, the dielectric constant, ε, being the classical bulk expression of this. In a small cluster there is little chance to delocalize the charge, simply because of the cluster's size. This means that charged clusters should be stabilized by a term of the form $E = -\frac{1}{2}(1 - \frac{1}{\varepsilon})\frac{q^2}{R}$, the self-energy of a charge in a finite space [23].

The radius, R, of the volume the charge is constrained within can be approximated by the Mott–Littleton radius, R_{ML}, of the cluster [24, 25]. The corrections to the energies of charged clusters are then given in table 3.

For example, in this approximation the process of placing a single charge on a $C_{10}H_{16}$ interstitial TM cluster is stabilized by 2.23 eV.

The simple model used to determine the charge stabilization gives an upper bound to the stability of the charged species. The stabilization will be over-estimated by this model for two reasons: because the model underestimates the size of the clusters, being based on the size of a unit cell of pure diamond, rather than the expanded lattice around a TM, and because it double-counts the effect of the near neighbours: they already provide some stabilization in the HF model by delocalizing the charge when forming MOs.

These large uncertainties in the absolute numbers make definite conclusions hard in many cases. The interstitial clusters are fairly clear cut, however. Even including the overestimated correction for finite cluster size, the negative charge states of the interstitial were found to be unstable relative to the neutral species by 5–7 eV (this was consistent between the different cluster sizes, where most of the charge is localized on the TM); negative interstitial clusters are unlikely to be found in diamond. Conversely, the positive charge states of TM_i were uniformly found to be stable, even without the dielectric screening correction. Interstitials are expected to be found in a positive charge state when a good acceptor species is present, but neutral in diamonds with significant nitrogen content (figure 7).

The results for the substitutional complexes are not as conclusive, being only 1–4 eV more stable on forming a charged species and compensating pair when the dielectric effect is included (see figure 8). It is of note, however, that Ni is found to be almost identically stable in both positively and negatively charged forms, given boron and nitrogen charge compensators respectively.

Semi-vacancy complexes show similar behaviour to the substitutional complexes (figure 9).

5. Optical properties

5.1. Interstitial

MCSCF calculations were carried out to optimize the lowest lying excited state obtained in the previous MCSCF calculations on the ground state of the complexes. The active space used was the five orbitals derived principally from the metal d orbitals.

The transition energies are shown in figure 10 (no transition energy is shown for Cr_i^+ as its ground $^6A_1$ state is the only sextuplet state that can be constructed within the d orbitals).

The TM_i complexes show a clear trend towards lower transition energies as the transition series is crossed and with positive charge on the TM: this is in agreement with the observed pattern of complexes with low-spin ground states. The other interstitial centres shown would be expected to have allowed transitions at slightly higher energies than Ni_i^+. Ni_i^0 is expected

Table 3. The Mott–Littleton radii of the clusters used in this paper and the approximate energy correction for placing a charge in the confines of the finite cluster.

Cluster	R_{ML} (Å)	Energy correction (eV)
C_5H_{12}	2.2	2.69
$C_{10}H_{16}$	2.7	2.23
$C_{27}H_{30}$	3.6	1.66
$C_{29}H_{36}$	3.7	1.58
$C_{43}H_{42}$	4.2	1.42

to have a transition at a much higher energy as the electron must be transferred to the metal 4s orbital.

5.2. Substitutional

The transition energy is found to peak at the closed shell species (Mn_s^-, Co_s^+ and Fe_s^0) and then drop (figure 11). The energies of transitions at the complexes that fit the vacancy model are at fairly similar energies, suggesting that the later TM_s species would be expected to appear at a similar position to Ni_s^-. The pattern of transition energies follows that of the separation between the highest partially occupied and lowest partially unoccupied orbitals. That the energies behave like this indicates that the one-electron orbital picture for the transitions is fairly respectable here. The wavefunctions are also well described by single determinant references. Whilst results should be regarded as essentially qualitative, the fact that they follow an explicable pattern suggests that they do approximate the real situation.

The transition energies are still found to be rather too high compared to the limited experimental evidence, Ni_s^- at 2.51 eV experimentally but at 4.59 eV from the calculations. The calculations suggest that Co_s^- would be observed at a similar energy to Ni_s^-, and that Fe_s^- and Cu_s^- would occur at marginally higher energies. The transition energies of the neutral clusters appear at energies about one electronvolt higher than the charged species. Ni_s^+ is expected to have a transition at a very similar energy to Ni_s^-.

5.3. Semi-vacancy

The large size of these clusters has precluded MCSCF calculations. However, a few qualitative points can be made. Because of the centre of inversion the Laporte selection rules mean that the allowed transitions are either going to be from the low energy TM-like orbitals to the partly filled di-vacancy like the e_u orbital, or from the e_u orbitals to the vacant metal states (see figure 5)—essentially charge transfer transitions. Without MCSCF calculations it is hard to estimate the magnitude of the di-vacancy–metal transitions. A good estimate of the $(a_{1g})^2(e_u)^3$–$(a_{1g})^1(e_u)^4$ metal–di-vacancy transition in Ni_{sv}^- can be made, however, at 0.7 eV. This line would be expected to be strong as it is fully allowed and overlap between the TM and the di-vacancy orbitals is large.

6. Conclusions

Whilst these calculations are, in many senses, inaccurate, several patterns are clearly evident that would not be so readily perceived if more detailed calculations were conducted on a smaller sample of the TMs.

The negative interstitial complexes are found to be unstable and unlikely to be formed. The neutral interstitial complexes have low-spin ground states; the crystal field splitting is

smaller for the positively charged interstitial complexes and they are generally found to be high spin. In accordance with the last two points, the transition energies of the interstitial clusters decrease across the transition series and are smaller for the positively charged clusters. The interstitial complexes are found to be less stable than the other two TM environments, suggesting that they are only metastable in diamond.

The LW and vacancy models of the TMs are only extremes. The substitutional TM defects move smoothly from the LW model at the beginning of the transition series to approximating the vacancy model for the later TM; some defects, notably Ni_s^-, are found to have electronic structures intermediate between the two models. The TM_s complexes are found to favour low-spin states. The transition energies of the later TMs are found to be quite similar, consistent with the transitions being between modified vacancy states. All charge states of TM_s appear to be of similar stabilities.

The semi-vacancy defects increase in stability across the transition series. They are found to be marginally less stable than TM_s at Ni but, including strain and entropy terms, Co and Cu might be stable, Fe is less likely. The orbitals of the metal and the di-vacancy cage appear to be of similar energy; which orbitals are occupied depends on electron–electron repulsions, and a good multi-configuration method is probably needed to be confident of a good description of the electronic structure of the TM_{sv} defects. These results suggest that unpaired electrons occupy the e_u orbitals derived from the di-vacancy dangling bonds. Again the charge states of TM_{sv} all appear to be of similar energy.

To obtain reliable calculations of chemical accuracy would require far more computationally expensive calculations than have been performed here: by checking results are consistent across a range of clusters and basis sets, and that results are in accord with chemical intuition, these calculations provide a useful tool for understanding the nature of TM defects in diamond.

References

[1] Paslovsky L and Lowther J E 1992 *J. Phys.: Condens. Matter* **4** 775
[2] Goss J, Resende A, Jones R and Oberg S 2001 *Mater. Sci. Forum* **67** 196
[3] Johnston K and Mainwood A 2000 *Physica* B **273/274** 647
[4] Johnston K and Mainwood A 2002 unpublished
[5] Iakoubovskii K and Stesmans A 2001 *Phys. Status Solidi* a **186** 199
[6] Baker J M 2001 *J. Phys.: Condens. Matter* **13** 2053
[7] Iakoubovskii K and Adrianssens G J 2002 *J. Phys.: Condens. Matter* **14** L95
[8] Zeitzev A M 2000 *Phys. Rev.* B **61** 12909
[9] Gippius A A and Collins A T 1993 *Solid State Commun.* **88** 637
[10] Nadolinny V A *et al* 1999 *J. Phys.: Condens. Matter* **11** 7357
[11] Schmidt M W *et al* 1993 *J. Comput. Chem.* **14** 1347–63
[12] Granovsky A A http://classic.chem.msu.su/gran/gamess/index.html
[13] Huzinaga S, Andzelm J, Klobukowski M, Radzio-Andzelm E, Sakai Y and Tatewaki H 1984 *Gaussian Basis Sets for Molecular Calculations* (Amsterdam: Elsevier)
[14] Hehre W J, Ditchfield R and Pople J A 1972 *J. Chem. Phys.* **56** 2257
[15] Wachters A J H 1970 *J. Chem. Phys.* **52** 1033
[16] Hehre W J, Stewart R F and Pople J A 1969 *J. Chem. Phys.* **51** 2657
[17] Hehre W J, Ditchfield R, Stewart R F and Pople J A 1970 *J. Chem. Phys.* **52** 2769
[18] Ludwig G W and Woodbury H H 1962 *Solid State Phys.* **13** 223
[19] Watkins G D 1983 *Physica* B+C **117B/118B** 9
[20] Coomer B J, Resende A, Goss J P, Jones R, Oberg S and Briddon P R 1999 *Physica* B **273/274** 520
[21] Kittel C 1997 *Introduction to Solid State Physics* 7th edn (New York: Wiley)
[22] Goss J P, Jones R and Briddon P R 2003 unpublished
[23] Sze S M 1981 *Physics of Semiconductor Devices* (New York: Wiley)
[24] Mott N F and Littleton M J 1970 *Trans. Faraday Soc.* **34** 2182
[25] Mott N F and Gurney R W 1940 *Electronic Processes in Ionic Crystals* (New York: Wiley)